Chapter 3

Bioadhesive chitosan NP

3. Bioadhesive chitosan nanoparticles for lung cancer therapy

3.1. Objective

The objective of this study is to design-optimize the targeting ability of docetaxel (DTX) loaded, cetuximab (CTX) decorated and TPGS stabilized chitosan nanoformulations and to evaluate their physicochemical, *in-vitro* release characteristics, *in-vitro* cellular uptake, cytotoxicity, apoptosis and wound-healing studies on A549 cells, *in-vivo* pharmacokinetics, histopathology studies in rats and *in-vivo* efficacy in B(a)P induced lung cancer mice model after *i.v.* administration. Results of CTX decorated targeted chitosan NP were compared to those of non-CTX decorated chitosan nanoformulation and the marketed DTX (Docel^{TM}) injection.

3.2. Plan of study

a. Formulation optimization by employing QbD approach

b. Preparation DTX loaded bioadhesive chitosan nanoparticles using solvent evaporation combined with ionic cross-linking method

c. Post-conjugation of CTX on the surface of DTX loaded chitosan nanoparticles using carbodiimide chemistry

d. *In-vitro* evaluation of CTX-conjugated chitosan nanoparticles

- Particle size, polydispersity index and zeta potential by DLS
- Electron microscopy (SEM, TEM & AFM)
- Crystallographic studies by XRD and surface composition by XPS
- Determination of entrapment efficiency
- *In-vitro* drug release studies
- *In-vitro* cellular bioadhesion and uptake study (qualitative & time-dependent) on A549 cells

- *In-vitro* cytotoxicity, apoptosis and wound healing studies on A549 cells
- *In-vitro* stability of nanoparticles on lyophilization, plasma and serum incubation and storage stability

In-vivo evaluation of CTX-conjugated chitosan nanoparticles

- Pharmacokinetic studies in Wistar rats
- Histopathology studies on Wistar rats
- Anticancer efficacy studies on B(a)P induced lung cancer mice model

3.3. Material

Docetaxel (99.56% pure) was a generous gift by Neon Labs. Docel^{TM} was procured from RPG, Mumbai. Cetuximab (Erbitux®) was supplied by Merck Specialities Ltd, Mumbai. High molecular weight chitosan was provided by SRL, Mumbai. TPGS was a liberal gift by Isochem, France. Sodium tripolyphosphate (Na-TPP) was purchased from Sigma-Aldrich, Bangalore. Dialysis membrane one kDa was purchased from Spectrum Laboratories Inc., CA, U.S.A. Fetal Bovine Serum, DMEM, PBS pH 7.4 and 3-(4,5-dimethylthiazol-2-yl)-2,5-diphenyltetrazolium bromide (MTT) were supplied by Himedia, Mumbai, India. 96-well culture plates and culture flasks of different capacities were obtained from Parsons Products, Kolkata, India. Trypsin-EDTA, antibiotic, and antimitotic penicillin-Streptomycin were supplied by Genetix Biotech Asia, Mumbai, India. Phalloidin-Tetramethyl rhodamine conjugate was provided by AAT Bioquest Inc., USA. All other reagents and chemicals used were of analytical quality.

3.4. Methods

In the development of DTX loaded chitosan nanoparticles (NP), Quality by Design (QbD) was employed which is a proactive, modern and scientific approach to product design and development [187,188].

3.4.1. Cause–effect relationship: Ishikawa fishbone

A risk assessment study was done by employing the Ishikawa fishbone diagram (figure 3.1) and the cause-effect relationship between the factors responsible and the critical quality attributes (CQAs) was configured by using failure mode and effects analysis (FMEA) (figure 1) [189-191]. With existing knowledge and expertise, particle size (PS), zeta potential (ZP), and entrapment efficiency (EE) were selected as key CQAs in the present study [192,193].

3.4.2. Risk assessment: Plackett–Burman design

The significant effect of identified risk factors on the mentioned CQAs was evaluated by Plackett–Burman design (PBD). The screening experiments with seven factors and three CQAs were performed initially with the highest and lowest levels of factors. With seven factors, three responses and 12 experiments, PBD was constructed using Minitab 19 software (Minitab, Inc., PA, USA), followed by statistical analysis (table 3.1) [194,195]. From the said experimental design, the observed CQA values are enlisted in table 3.1. The significance of PBD and the coefficients for each factor were evaluated by applying analysis of variance (ANOVA). Further, the key factors that influence CQAs (responses) on a large scale were selected by employing the Pareto charts (figure 3.2) [196,197].

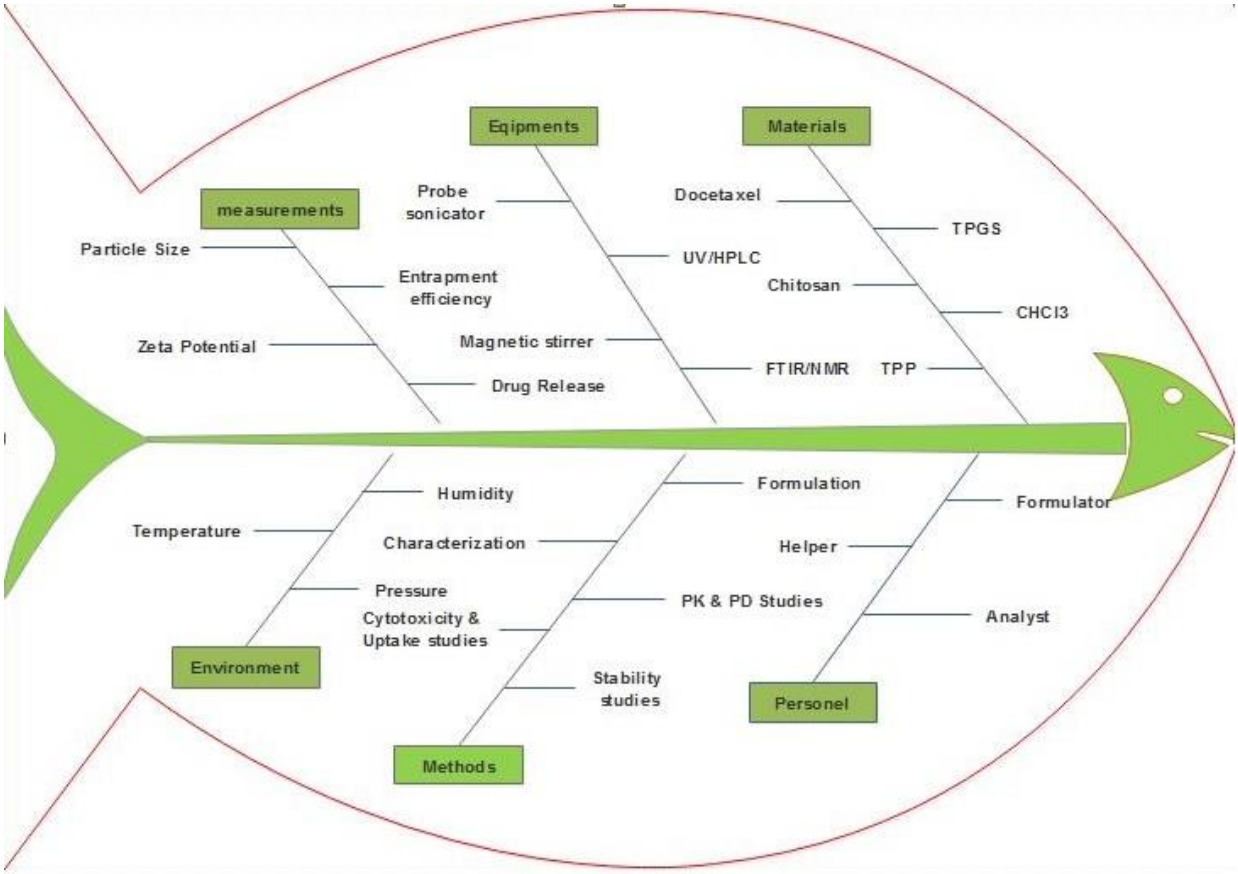

Critical Quality Attributes (CQAs, responses)	Critical Process Parameters (CPPs, Factors)						
	X_1: Polymer Concentration	X_2: Temperature	X_3: Crosslinker Concentration	X_4: TPGS Concentration	X_5: Sonication Time	X_6: Stirring Speed	X_7: Stirring Time
Y_1: Particle size	High	High	Medium	Low	Medium	Medium	Low
Y_2: Zeta Potential	Medium	High	High	Medium	Low	High	Medium
Y_3: Entrapment Efficiency	High	Medium	High	Medium	Medium	Low	Low

Figure 3.1. Ishikawa fishbone diagram showing the cause-effect relationship between variables for the critical quality attributes of DTX loaded chitosan nanoparticles and risk analysis by failure mode and effects analysis (FMEA) method

Table 3.1. Composition of DTX loaded chitosan NP with the levels of various factors and the results of observed mean values of various responses by Plackett–Burman design. & list of the selected three factors and their levels for the 3^3 full factorial design along with the responses.

Run	X_1	X_2	X_3	X_4	X_5	X_6	X_7	Y_1*	Y_2*	Y_3*
PBD-1	-	+	-	-	-	+	+	277±09.02	17.25±0.26	78.35±1.23
PBD-2	+	-	-	+	-	-	-	314±08.60	13.61±0.95	65.41±2.13
PBD-3	-	-	-	+	+	+	-	179±10.54	11.26±0.88	61.52±1.66
PBD-4	-	-	-	-	-	-	-	195±07.48	09.08±0.32	65.34±2.29
PBD-5	+	+	-	+	+	-	+	343±06.53	18.69±0.34	74.38±3.33
PBD-6	+	-	+	-	-	-	+	384±07.84	06.54±0.73	76.14±3.21
PBD-7	-	+	+	+	-	+	+	392±11.26	14.52±1.02	74.11±2.03
PBD-8	+	+	+	-	+	+	-	397±14.81	19.23±0.27	80.92±3.68
PBD-9	-	-	+	+	+	-	+	283±07.93	06.2±01.01	67.25±3.67
PBD-10	+	-	-	-	+	+	+	345±17.20	11.42±1.22	76.48±1.83
PBD-11	+	-	+	+	-	+	-	388±10.78	10.38±1.60	74.71±2.92
PBD-12	-	+	+	-	+	-	-	312±08.57	12.79±0.96	78.51±3.48

Independent Variables (factors)	**Name**	**Unit**	**Minimum**	**Maximum**
X1	Polymer Concentration	mg/10 ml	10	50
X2	Temperature	℃	10	40
X3	Crosslinker Concentration	mg/10 ml	2	8

Dependent Variables (responses)	**Name**	**Unit**	**Constraint**	**Dependent Variables (responses)**
Y1	Particle Size	nm	Minimize	Y1
Y2	Entrapment Efficiency	%	Maximize	Y2
Y3	Zeta Potential	mV	Maximize	Y3

*Mean ± standard deviation, n = 3

+: High level,
−: Low level;
X_1 : Polymer Concentration;
X_2 : Temperature;
X_3 : Crosslinker Concentration;
X_4 : TPGS Concentration;
X_5 : Sonication Time; X_6 : Stirring Speed
X_7 : Stirring Time;
Y_1 : Particle size;
Y_2 : Zeta Potential;
Y_3 : Entrapment Efficiency

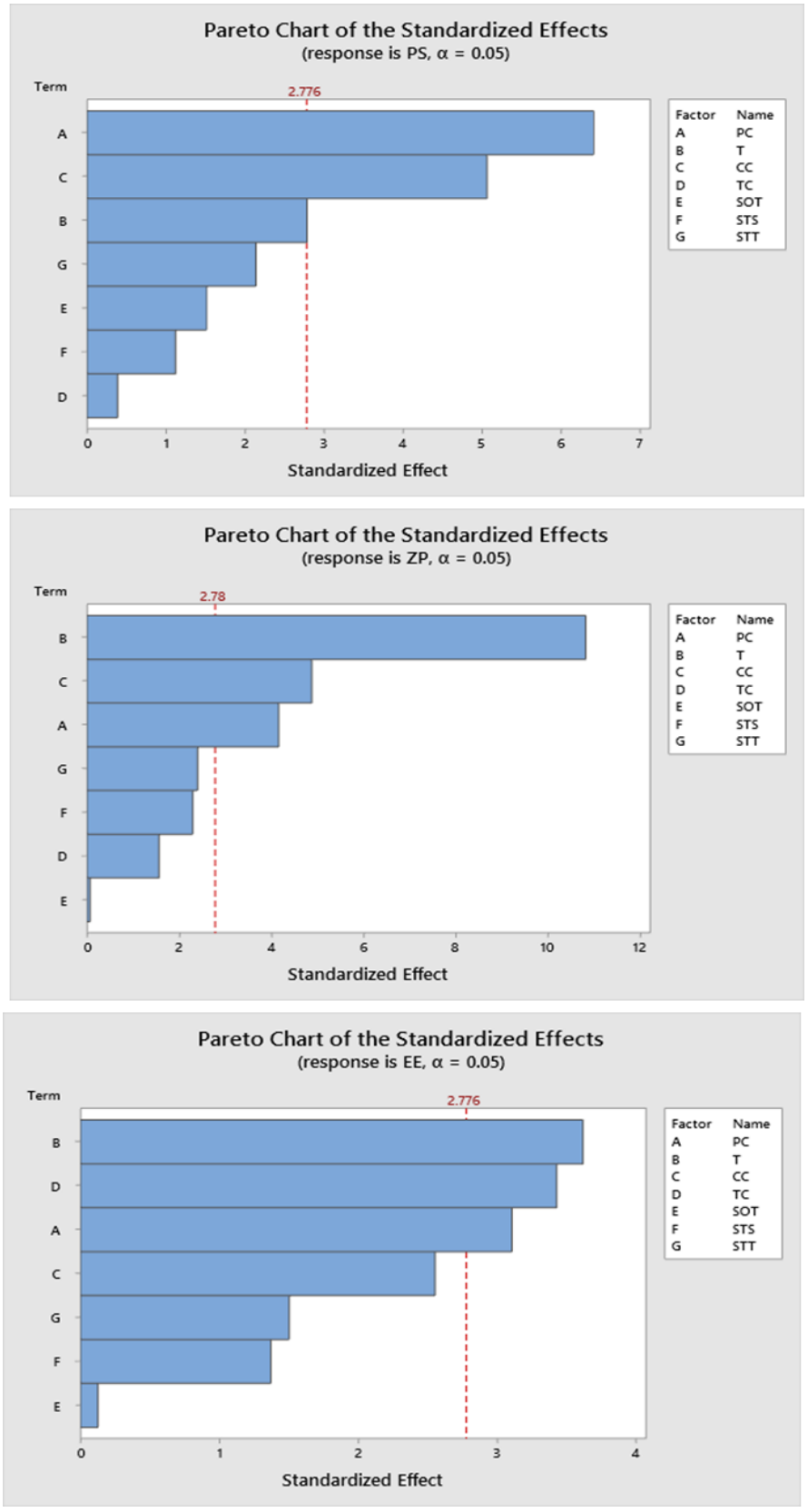

Figure 3.2. Pareto charts showing the influence of significant factors on responses (particle size, zeta potential and percentage entrapment efficiency) of DTX loaded chitosan NP.

3.4.3. Optimization of nanoformulation: 3^3 factorial design

The effect of three main factors (polymer concentration [PC], temperature [T], and crosslinker concentration [CC]) on the critical responses (PS, ZP, and EE) was evaluated. A 3^3 factorial design (FD; 3-factor, 3-level) was applied to optimize the DTX-CS-TPGS-NPs (table 3.2) in terms of the small size with narrow distribution; higher surface charge for better stability and efficient drug loading to reduce the dose and related side effects [198]. The experimental design was constructed and evaluated by using Minitab 19 software. Fifteen batches were prepared as per FD and their compositions were presented in table 3.2. To determine the significance of the experimental model, ANOVA was employed [199].

The polynomial equation generated by FD, elucidating the effect of factors on each of the responses is as follows:

$$Y_r = \delta_0 + \delta_1 X_1 + \delta_2 X_2 + \delta 3\ X_3 + \delta_{12} X_1 X_2 + \delta_{13} X_1 X_3 + \delta_{23} X_2 X_3 + \delta_{123} X_1 X_2 X_3$$

3.4.4. Nanoparticle preparation

For NP preparation, solvent evaporation combined with ionic cross-linking, with some modifications, was used [200]. Briefly, chitosan (30 mg) was solubilized in 0.2% (v/v) acetic acid (2 ml). Using a dilute sodium hydroxide solution, the pH was brought down to 6. Following, 1 ml chloroform containing TPGS and DTX (20 mg, 3 mg) was added to the above chitosan solution and emulsified by ultrasonic probe sonicator. The resulting nanoemulsion was agitated for 7 h to eliminate chloroform leaving the drug precipitated within the chitosan nano matrices. At this stage, the addition of sodium tripolyphosphate (NaTPP) solution (0.5mg/ ml, 2.5 ml) instigated cross-linking of chitosan polymer chains which makes NP robust. The resulting NP were centrifuged at 3,000 rpm for 10 min and the settled larger particles were discarded. One more centrifugation was carried out at

17000 rpm for 15 min to pellet out desired NP following which the clear afloat fluid was discarded.

Table 3.2. The 3^3 factorial design matrix and results of observed mean values of various responses & the predicted and the actual values of the selected responses considered for optimized formulation FD7

Run Order	**X_1**	**X_2**	**X_3**	**Y_1 ***	**Y_2***	**Y_3***
FD-1	30	25	5	165.26±3.76	12.68±0.43	69.74±2.39
FD-2	30	10	2	159.54±3.69	11.14±0.91	68.82±4.02
FD-3	30	40	2	160.61±4.37	11.26±1.06	69.28±4.21
FD-4	10	25	2	148.25±6.67	11.02±0.86	62.84±2.71
FD-5	10	10	5	150.42±6.82	12.18±1.51	64.22±3.00
FD-6	30	40	8	176.92±3.72	13.24±1.23	77.68±2.44
FD-7	30	25	5	166.74±5.38	12.88±1.10	70.15±2.96
FD-8	50	10	5	172.36±3.79	12.49±0.58	73.24±3.57
FD-9	50	25	2	178.52±2.94	11.63±0.32	72.42±2.40
FD-10	50	25	8	180.63±5.21	13.84±0.93	74.20±3.18
FD-11	50	40	5	170.88±8.53	12.92±1.58	70.66±2.76
FD-12	10	40	5	152.59±3.90	12.4±01.04	65.26±3.70
FD-13	30	10	8	163.64±4.28	13.12±1.27	72.48±3.68
FD-14	30	25	5	166.25±6.43	12.56±0.59	70.04±3.44
FD-15	10	25	8	158.44±6.81	13.04±0.71	72.44±2.45

Selected factors for optimization of responses		
Independent Variables (Factors)	**Results obtained from Factorial Design**	
X1-Polymer Concentration (mg)	30 mg	
X2-Temperature (°C)	25 °C	
X3-Crosslinker Concentration (mg)	5 mg	
Dependent Variables (Responses)	**Predicted value**	**Observed value**
Y1-Particle Size (nm)	166.74± 5.38	180.73 ± 0.997
Y2-Zeta Potential (mV)	12.88 ± 1.10	16.4 ± 1.327
Y3-Entrapment Efficiency (%)	70.15 ± 2.96	74.42 ± 0.576

*Mean ± standard deviation, n = 3

X_1 : Polymer Concentration; X_2 : Temperature; X_3 : Crosslinker Concentration; Y_1 : Particle size; Y_2 : Entrapment Efficiency; Y_3 : Zeta Potential

The settled NP were cleared of the excess unentrapped drug by washing for three times with distilled water. The resulting pellet was dispersed in distilled water using vortexer to get a homogenous suspension of NP.

In the case of targeted NP, a similar procedure was followed except that a mixture of TPGS-COOH and TPGS (15 mg, 5 mg respectively) was used instead of 20 mg of TPGS [201]. Activation of the resulting NP was carried out with the help of EDC and NHS for the conjugation of CTX onto their surface so as to prepare targeted formulation [202]. Then, 0.5 ml of Erbitux (CTX 5mg/ ml) was added to the activated NP and a brief stirring for 30 min facilitated CTX surface conjugation. The prepared non-targeted and targeted NP were then dialyzed against a saturated DTX solution using 1 kDa membrane to make them free of the unentrapped drug.

3.4.5. NP characterization

3.4.5.1. Solid-state characterization by X-ray diffraction (XRD)

XRD was performed to observe the physical properties of drugs and excipients in their pure form and the formulation to check the crystallinity as well as any change in the drug's physical state after the entrapment [203]. The XRD spectra of non-targeted, targeted formulations and the pure drug were obtained by using SmartLab (Rigaku, Japan) diffractometer. The diffractograms were recorded by using 15 mA amperage, 40 kV tube voltage, 10° min^{-1} scan speed, 0.02° step width, and 20°–80° 2θ scanning range [204].

3.4.5.2. Surface chemistry by X-ray photon correlation spectroscopy (XPS)

The surface chemistry of targeted and non-targeted NP was determined using the XPS survey (K-Alpha, Thermo Fisher Scientific). Samples were prepared by placing a drop of NP suspension on a glass slide and drying for 12 h. Various characteristic peaks for carbon, nitrogen, and oxygen were observed at their corresponding binding energy ranges such as 280-290, 530-535, and 398-403 eV, respectively.

3.4.5.3. Physicochemical characterization

Prepared NP were characterized for particle size, ploydispersity index and zeta potential by DLS (dynamic light scattering, Malvern Zetasizer Nano S90) at 25 °C [205,206]. A five times dilution of prepared NP was made with millipore water before evaluation. Three independent analyses (n=3) were done to arrive at the mean value.

3.4.5.4. Scanning electron microscopy (SEM)

The visualization of the surface architecture of the prepared NP was carried out by using SEM. The microscope was set at a 50,000X magnification level. The NP were diluted up to 5 times with ultra-pure water, spread evenly on glass slides and subjected to drying under vacuum. The sample slides were coated with carbon to make them conductive and then the micrographs were obtained [207].

3.4.5.5. Transmission electron microscopy (TEM)

The surface conformation of prepared nanoformulations was observed by TEM. Ten times dilution of prepared NP was made with ultra-pure water and tiny drops of the prepared NP were placed on separate carbon-coated copper grids and dried under vacuum. The micrographs were acquired with TEM at 80 kV [208].

3.4.5.6. Atomic force microscopy (AFM)

The surface texture of prepared NP was observed by using an AFM (Solver P-47-PRO, MDT; Moscow, Russia) [200]. The processing of data was done by AFM image analysis software.

3.4.5.7. Estimation of entrapment efficiency

The DTX entrapment efficiency of the prepared NP was estimated by HPLC [37]. Briefly, a 1 ml NP suspension was pelleted (ultra-centrifuge, 17000 rpm) and the clear afloat fluid was aspirated out. The pelleted NP were uniformly dispersed in millipore water. A small

aliquot of the resulting dispersion was evaporated in a small RBF using a rotary evaporator. The residue was dispersed in methanol and agitated on a vortexer for 24 h. The resulting solution was again centrifuged at 10,000 rpm. The clear supernatant was aspirated out, filtered through a membrane filter (0.45 µm) and analyzed by RP-HPLC at 230 nm. The entrapment efficiency was computed as

Entrapment efficiency (%) = (DTX entrapped within the NP/ total amount of DTX used in the preparation) x 100

3.4.5.8. The extent of CTX conjugation

The extent of CTX conjugation onto the surface of targeted NP was determined by Bradford assay [175]. Briefly, 1ml of each of non-targeted, targeted formulations and blank PBS pH 7.4 were treated with 5ml Bradford reagent for 5 min and then the UV absorbances were recorded. The extent of CTX conjugation was computed from the calibration curve constructed from serial dilutions of bovine serum albumin (BSA). The equation to determine the extent of conjugation was

$$\text{Extent of CTX conjugation} = \frac{\text{CTX amount in targeted NP} - \text{CTX in non-targeted NP}}{\text{Amount detected in standard CTX solution}}$$

3.4.6. In-vitro studies

3.4.6.1. Drug release studies

The trend of DTX release from prepared formulations was explored by dialysis using a 5 kDa membrane [209]. An accurate 1 ml aliquot of NP suspension (~0.3 mg DTX) was sealed in the dialysis membrane and placed in a beaker containing buffer (50 ml, pH 7.4, and pH 5.5), maintaining a constant temperature of 37 ± 0.5 ℃ and magnetically stirring at 100 rpm. At predetermined time intervals, 15 ml of release media was collected and replaced again with fresh media to maintain sink condition. Finally, the collected aliquot at each sampling point was analyzed for the drug concentration by RP-HPLC at 230 nm.

3.4.6.2. Cellular bioadhesion study

To study the bioadhesive character of non-targeted and targeted NP, A549 human lung cancer cells (5×10^4 per well) were seeded in a 6-well plate in 1x PBS and subsequent treatment was done with non-targeted and targeted formulations (0.5 ml, 0.3 mg of DTX/ ml) in separate wells for 1 h. Following, from each of the wells, a drop of NP-treated cell suspension was mounted on separate coverslips and subsequent fixing was done with PBS stabilized glutaraldehyde solution followed by dehydration with alcohol various dilutions (50 to 100%) and then dried in ambient temperature. These coverslips were then micrographed with SEM [210].

3.4.6.3. Cellular uptake study

A549 cell line was separately seeded into a 6-well plate at a count of 1×10^5 cells per each well. After 24 h, the cells were incubated with free coumarin-6 (CM6) and CM6 loaded NP for 2 h. CTX pre-treatment was done to one of the wells to check the definitive role of EGFR in the uptake of CTX decorated targeted NP. After a specified time, the medium along with the formulations was withdrawn from the wells, followed by PBS washing of cells. After routine fixation with 4 % formaldehyde, nuclear staining was done with 4′,6-diamidino-2-phenylindole (DAPI) for 15 min and then, cells were observed under a fluorescence microscope to evaluate the NP uptake [211]. The mean fluorescence intensity produced by cells after treatment with free CM6, CM6 loaded non-targeted and targeted NP was computed by using ImageJ® software.

3.4.6.4. Time-dependent cellular uptake study

For this, CM6 loaded formulations and free CM6 (5µg/ml) in DMEM were added into the 6 well plates previously seeded with around 5×10^5 cells per well. The cells were observed under a fluorescence microscope [175,209] at various time points immediately

post-treatment such as 0, 15, 30, and 60 min respectively after removing the medium containing formulations and free CM6 and washing with PBS.

3.4.6.5. Cytotoxicity study in A549 cells

The cytotoxicity of the prepared nanoformulations and Docel^{TM} (standard) on A549 human lung carcinoma cells was evaluated by MTT assay. For this, A549 cells were plated into 96 well plate and subsequent incubation, for 12h, was done to facilitate the appropriate cell adhesion which is a characteristic of solid tumors. The cells were then incubated with both non-targeted and targeted NP and Docel^{TM} in DMEM and the cytotoxicity was assessed at various dilutions (0.025, 0.25, 2.5, and 25 µg/ml of DTX) for 24 h. Following, the exhausted medium containing treatments was replaced with 100 µl of fresh DMEM along with 10 µL of 3-(4,5-dimethylthiazol-2-yl)-2,5-diphenyltetrazolium bromide (MTT) in PBS in each well of the plate. Incubation was again done for 2 h, after which the medium along with MTT, was discarded. Subsequently, the addition of 100 µL of DMSO to each well and gentle shaking on a gyratory shaker for 5 min was done to ensure complete dissolution of resulting formazan crystals. The optical density was then computed at 570 nm using a microplate reader. Cytotoxicity was assessed for the treated cells and normalized with the readings observed from the untreated cells [212]. The % cell viability was determined as;

Cell viability (%) = (Absorbance from treated cells/Absorbance from control cells) x 100

3.4.6.6. Wound-healing assessment

A549 cells were seeded in a 6-well plate at a population of 5x 10^4 per well and incubated until proper attachment of cells as monolayers. The cell monolayers were then scratched horizontally and vertically as a cross with a sterile 100 µl micropipette tip followed by washing with 1xPBS three times and then incubated in a fresh serum-free DMEM with

or without nanoformulations for 24 h. The trend of migration and wound healing of the scratched area of the cells were observed under an inverted microscope and microphotographed from 0 to 48 h and the extent of cell migration in terms of percent scratch area covered within 48 h was evaluated [213].

3.4.6.7.Cellular apoptosis study

After incubation of A549 cells at 37 °C for 24 h in a 6-well plate for proper cell adhesion, both the formulations and Docel^{TM}, at DTX concentration being equivalent to IC_{50} value, were added to the cells and incubated again for 2 h. After the specified time, routine fixing with 4% paraformaldehyde in PBS (pH 7.4) was done and nuclear staining with DAPI and F-actin counter staining with 1X phalloidin tetramethyl rhodamine conjugate in PBS with 1% BSA at room temperature were done for 5 min and 30 min respectively. Then, the cells were washed twice with ice-cold PBS [214,215]. Stained cells were visualized under the fluorescent microscope (OLYMPUS, IX 71, Japan).

3.4.7. Stability studies of prepared nanoformulations

3.4.7.1. Freeze-drying & reconstitution

The possible impact of lyophilization and subsequent reconstitution on the size and surface charge of prepared nanoformulations was evaluated in this study. After preparation, formulations were freeze-dried and the resulting free-flowing solids were stored in air-tight glass vails. Following, the lyophilized specimens were reconstituted with PBS pH 7.4 and then evaluated for any changes in particle size, size distribution, and surface charge [216,217].

3.4.7.2. Stability in plasma

The effect of plasma on the stability of prepared formulations was analyzed in this study. Freshly prepared NP suspensions were incubated for a brief time (12 h) with equal

volumes of rat plasma at 37 ℃. Following, the incubated samples were separated from plasma and investigated for any change in particle size, size distribution, and surface charge [218].

3.4.7.3. Stability in serum

The *in-vivo* dynamics of NP were predicted by incubation with rat serum for a definite time followed by analysis for any change in particle size, size distribution, and surface charge [219]. Briefly, nanoparticle suspensions were added with equal with rat serum, incubated for 6 h at 37 ºC under gentle agitation. The NP were then separated from serum and evaluated for any change in particle size, size distribution, and surface charge.

3.4.7.4. Effect of storage

The possible impact of brief storage at different temperatures on the stability of freeze-dried NP was analyzed in terms of change in size, size distribution, and surface charge in this study [220]. The freeze-dried specimens of NP were sealed in glass vials and stored at cold (4 ºC) and room temperatures (25 ºC). At preidentified time intervals (7, 15, and 30 days), samples were taken from these vails and analyzed for the said parameters.

3.4.8. In-vivo studies

3.4.8.1. Pharmacokinetics study in rats

Wistar rats (male and female, 4–5 weeks) were procured and housed at ambient conditions of 37 ℃ and 50–60% RH and a complete nutritional feed and sterile water were provided for at least 7 days before initiating any studies (Central Animal Ethical Committee approval number: Dean/2019/IAEC/1245). Following, rats were randomly segregated into four groups, with four rats in each group (n=4). Intravenous injection of normal saline was given to group 1 which served as control. Docel^{TM} (as drug control) was given to group 2 via the lateral tail vein. Non-targeted NP to group 3 and targeted NP to group 4

were administered in normal saline (7.5 mg of DTX/kg of body weight). At prespecified time points (0.5, 1, 2, 4,8, 12, 24, and 48 h), 0.5 ml blood was drawn out from different groups (group 1-4) of rats through the tail vein. Centrifugation of collected blood samples at 11,000 rpm for 10 min was performed to separate plasma and the same were stored at -20 ºC until further analysis by HPLC [221].

For HPLC analysis, extraction of DTX was carried out from 0.1 ml plasma samples into 1 ml ethyl acetate and the later was allowed for evaporation. Then, the residue in the tubes was added with 100 µl of mobile phase B (acetonitrile:water: methanol-55:40:5) and vortexed for 10 min followed by centrifugation for 15 min at 10,500 rpm. The clear supernatant was collected and 90 µl of the same was aliquoted into HPLC vials. Then, the protocol was set in such a way that the flow rate was 1 ml/min and the sample volume injected was 50 µl. Gradient elution was carried out by changing the proportion of mobile phase A (acetonitrile:water: methanol = 50:45:5) from 0 to 100% and then again brought back to 100% B in 50 min and then maintained for 4 min at 100% B with the total run time being 55 min. The standard calibration curve was used to quantify the DTX concentration in plasma samples [222].

3.4.8.2. Histopathology study in rats

After administration of saline, standard, non-targeted and targeted formulations (multiple dosing of 7.5 mg/kg) to separate groups of rats, once in every 3 days and for 3 times, animals were euthanized on 15th day and then the vital organs like lungs, liver, kidneys and heart were collected and washed with normal saline followed by fixing with 10% formalin and then paraffin blocking was done. After routine processing, paraffin sections of a 5 µm thick were mounted on separate glass slides. The above sections were treated

with hematoxylin & eosin (HE) for cytoplasmic contrast microscopy and then visualized under a microscope for histopathological findings [223,224].

3.4.8.3. Evaluation of anticancer efficacy of NP

The Swiss albino mice were segregated into five groups with each group consisting six mice. Group I was designated as negative control and was administered with olive oil orally for four weeks. Group II animals were treated with benzo(a)pyrene ((B(a)P) 50 mg/kg body weight dissolved in olive oil orally) weekly twice for 4 weeks, to induce lung cancer by 16^{th} week, which serve as model control. Group III animals were treated with non-targeted NP (i.v., 7.5 mg DTX/kg body weight) for 4 weeks after they were treated with the first dose of B(a)P (as in Group II). Group IV animals were treated with targeted NP (as in G-III) for 4 weeks after they were treated with B(a)P). The induction of lung cancer was confirmed by histopathological study. Group V animals were treated with standard Docel for 4 weeks to study the cytotoxicity (if any) induced by DTX after they were treated with B(a)P. Food and water will be available *ad libitum*. During the study, the health conditions of mice were monitored every day, and the body weights were measured every week. Survival analysis was done by applying Kaplan-Meier survival curves to compute percent survival [225]. After 16 weeks, the mice were anesthetized intraperitoneally with urethane (2 g/kg body weight) and then sacrificed. Subsequently, the lungs were dissected, fixed with 10% formalin and then paraffin blocking was done. After routine processing, paraffin sections of a 5 µm thick were mounted on separate glass slides. The above sections were treated with hematoxylin & eosin (HE) and these sections were analyzed for cancer cell numbers by using ImageJ software [226,227].

3.4.9. Statistical analysis

Mean values (n=3) of particle size, entrapment efficiency, etc., were correlated using the One-way ANOVA. Differences are deemed significant at $P<0.05$.

3.5. Results & discussion

3.5.1. Risk identification & risk assessment screening

From risk assessment studies, PC, T, and CC were identified as significant variables that influenced the responses through preliminary screening by PBD (table 3.1) and; PS, ZP and EE were selected as responses (table 3.1). Pareto charts for PS, ZP, and EE are shown in figure 3.2. ANOVA was employed to evaluate the significance of PBD and statistically significant coefficients for each factor.

3.5.2. 3^3 Factorial design

The mean PS of the optimized nanoformulation developed according to the 3^3 FD was in the range of 152.59±3.90 nm to 180.63±5.21 nm (table 3.2). The polynomial equation generated by the FD showing the effect of factors on PS was as follows:

Y1=22.7 + 2.412 PC + 1.530 T + 12.70 CC + 0.194 TC - 3.80 SOT + 0.0337 STS + 0.358 STT.

The ZP of the optimized nanoformulation developed according to the 3^3 FD was in the range of 11.02 ± 0.86 mV to 13.84 ± 0.93 mV (table 3.2). The polynomial equation generated by the FD showing the effect of factors on ZP is as follows:

Y2 = -6.62 - 0.0696 PC - 0.2644 T + 0.544 CC - 0.0349 TC - 0.008 SOT - 0.00307 STS + 0.01789 STT.

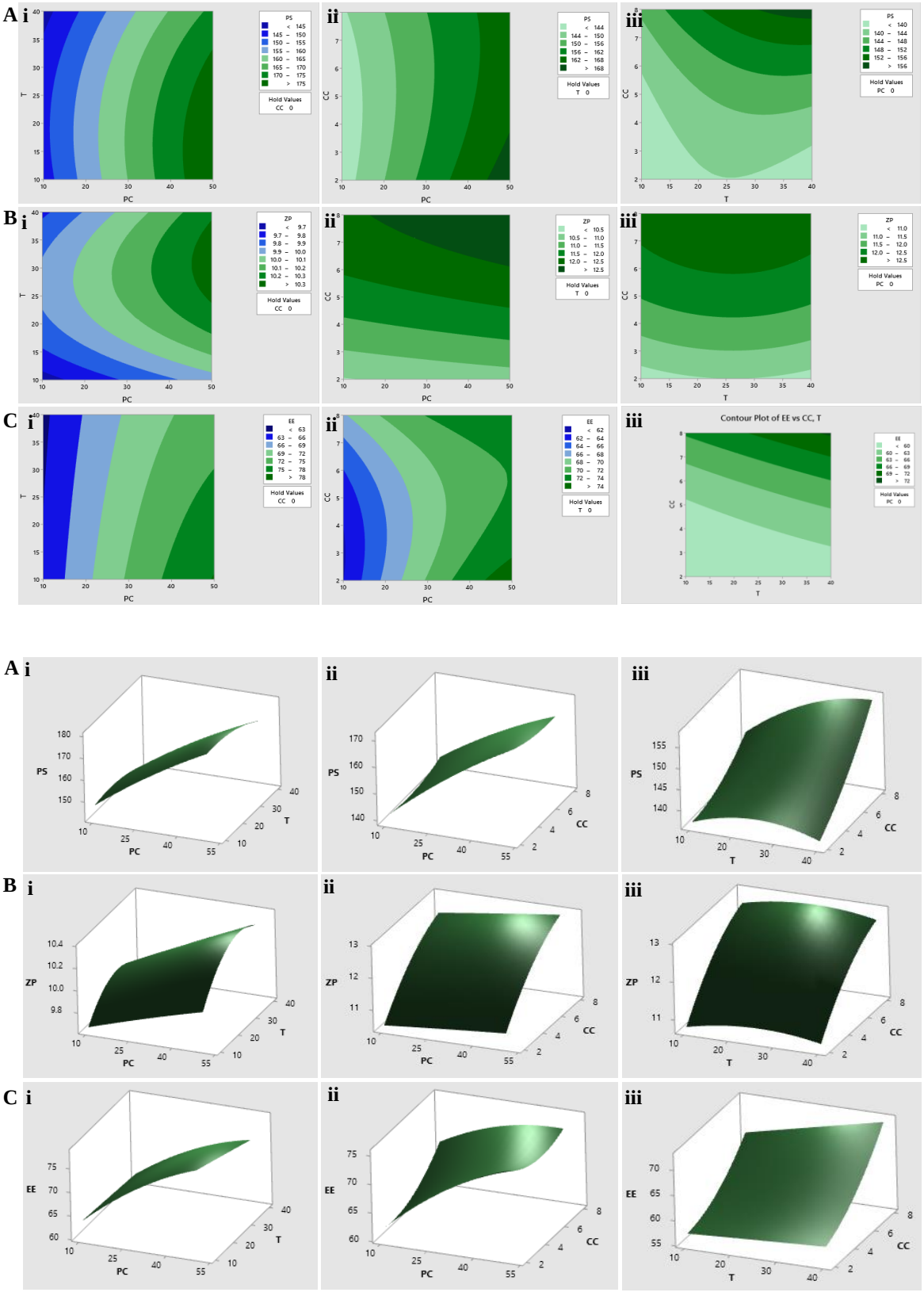

Figure 3.3. The 3D response surface plots and the contour plots showing the effect of polymer concentration (PC), temperature (T) and crosslinker concentration (CC) on particle size [A & D] , zeta potential [B & E] and % entrapment efficiency [C & F] respectively.

The EE of the optimized nanoformulation developed according to the 3^3 FD was found in the range of 62.84 ± 2.71 to 77.68 ± 2.44 (table 3.2). The effect of factors on EE is expressed by the polynomial equation generated through the FD as shown below:

Y3 = 62.31 + 0.1215 PC + 0.2066 T + 0.666 CC - 0.1787 TC - 0.033 SOT + 0.00429 STS + 0.0261 STT

The 3D response surface plots of the optimized nanoformulation and corresponding contour plots are shown in figure 3.3. The quadratic model's ANOVA analysis generated for all the three rsponses indicated no lack of fit (>0.05) between predicted values and experimental results, and thus the model can be used to plot the optimized design space.

3.5.3. NP characterization

3.5.3.1. Solid-state characterization by XRD

The XRD analysis of pure DTX, DTX loaded non-targeted and targeted formulations was performed and the results are shown in figure 3.4.i. The XRD analysis of pure DTX has revealed the crystalline nature in its spectrum through the presence of numerous peaks; these peaks were absent in the spectra of both the prepared NP. This indeed validated the fact that DTX was entrapped in an amorphous form with in the formulations.

3.5.3.2. Surface chemistry by XPS

The elemental constitution of C, N, O on the surface of the non-targeted and targeted NP was ascertained by XPS. The results are shown in figure 3.4.ii, from which it is evident that for both the formulations, XPS wide scan revealed N 1s signal at 398 eV; C 1s and O 1s peaks were visible at 285 eV and 532 eV respectively. Here, non-targeted NP, at the N1s binding energy region, revealed a low-intensity peak due to the N element of the amino groups, which are present in the polymer backbone of the chitosan. But, with the targeted NP, an intense peak was observed due to the additional nitrogen from the anti-

EGFR antibody CTX that was conjugated on the outer surface of the targeted NP. This indeed proved the conjugation of CTX on to the surface of targeted NP.

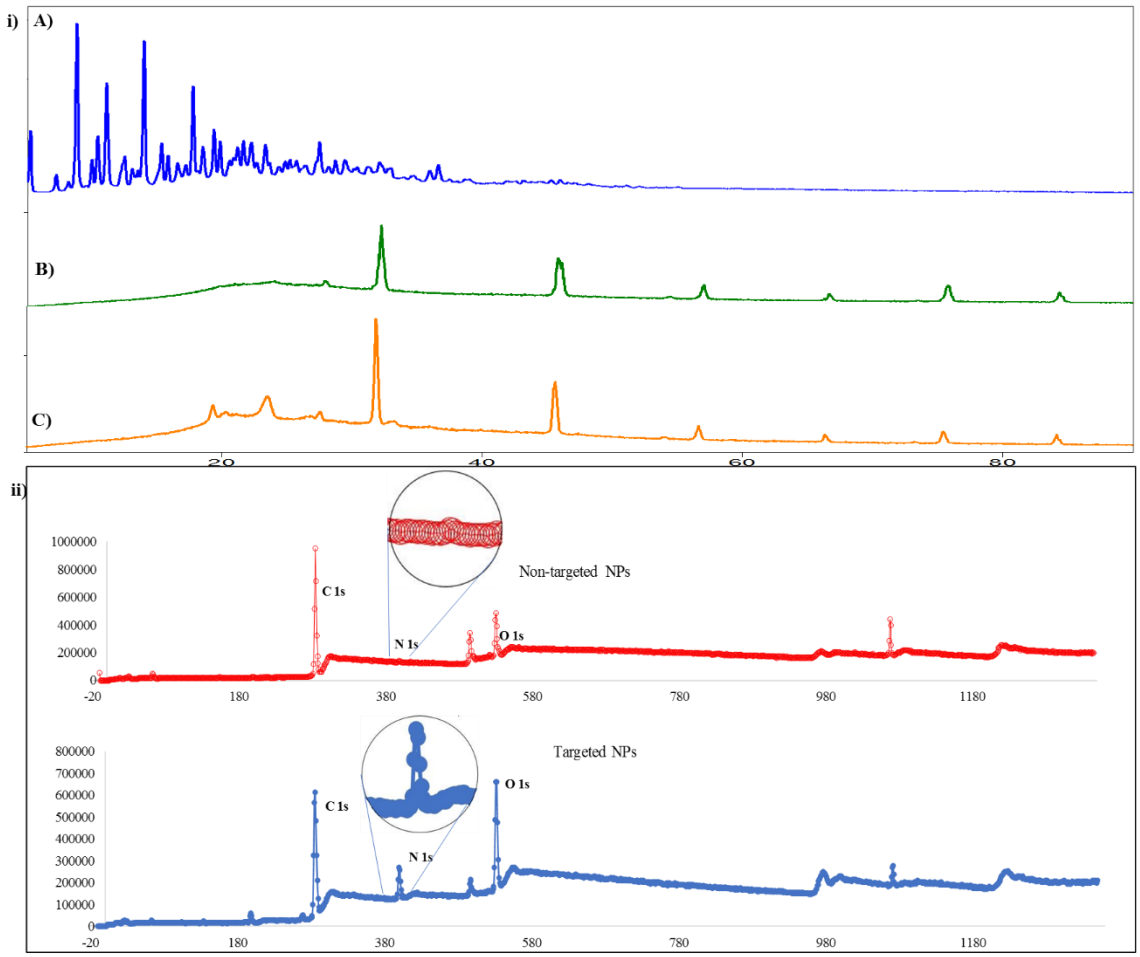

Figure 3.4. i) XRD overlay spectrum of pure DTX and non-targeted and CTX decorated targeted NP; **ii)** XPS spectra of non-targeted and CTX decorated targeted NP.

3.5.3.3. Electron microscopy (SEM, TEM & AFM)

The micrographs of the non-targeted and targeted NP from SEM (figure 3.5. A&B) and TEM (figure 3.5. C&D) revealed that the NP are more or less spherical and are in the range of 210 nm in size. The NP with this size range are most suitable to achieve EPR effect through leaky vasculature of cancer tissue. Moreover, there was an excellent agreement between the particle size data obtained from zeta sizer and that of electron microscopy studies. The AFM 3D micrographs of non-targeted, and EGFR targeted NP

(figure 3.5. E&F) revealed the smooth surface of NP which are devoid of any holes or defects. These images even confirmed the fact that the TPGS-COOH coated NP were also spherical with sizes lesser than 210 nm.

3.5.3.4. Bioadhesion study of NP

The bioadhesive behavior of nanoformulations was studied in A549 human lung adenocarcnoma cells and the images (figure 3.5 G&H) revealed no significant change in morphology or surface attachment of NP. The formulated NP have adhered, in huge numbers, to the surface of A549 cells that possess a negative surface charge, possibly due to bioadhesive nature of chitosan in addition to the receptor mediated binding and endocytosis.

3.5.3.5. Drug entrapment efficiency

The entrapment efficiency of the non-targeted NP was found to be 70.8 ± 0.812 %. But, the entrapment efficiency of DTX within the targeted NP was found to be 74.42 ± 0.576 % (table 3.3). The surface conjugation of CTX on the targeted NP resulted in a marginal increment in the entrapment efficiency of DTX. The CM6 entrapment efficiency within the CM6-CS-TPGS- NP, and CM6- CS-TPGS-CTX-NPs was found to be 84.0 ± 1.56 % and 88.6 ± 2.36 % respectively.

3.5.3.6. The extent of CTX conjugation

The extent of CTX conjugation onto the sutface of DTX loaded and C6 loded targeted NP by Bradford assay was found to be 78.44±3.65 % and 75.81±5.67 % respectively.

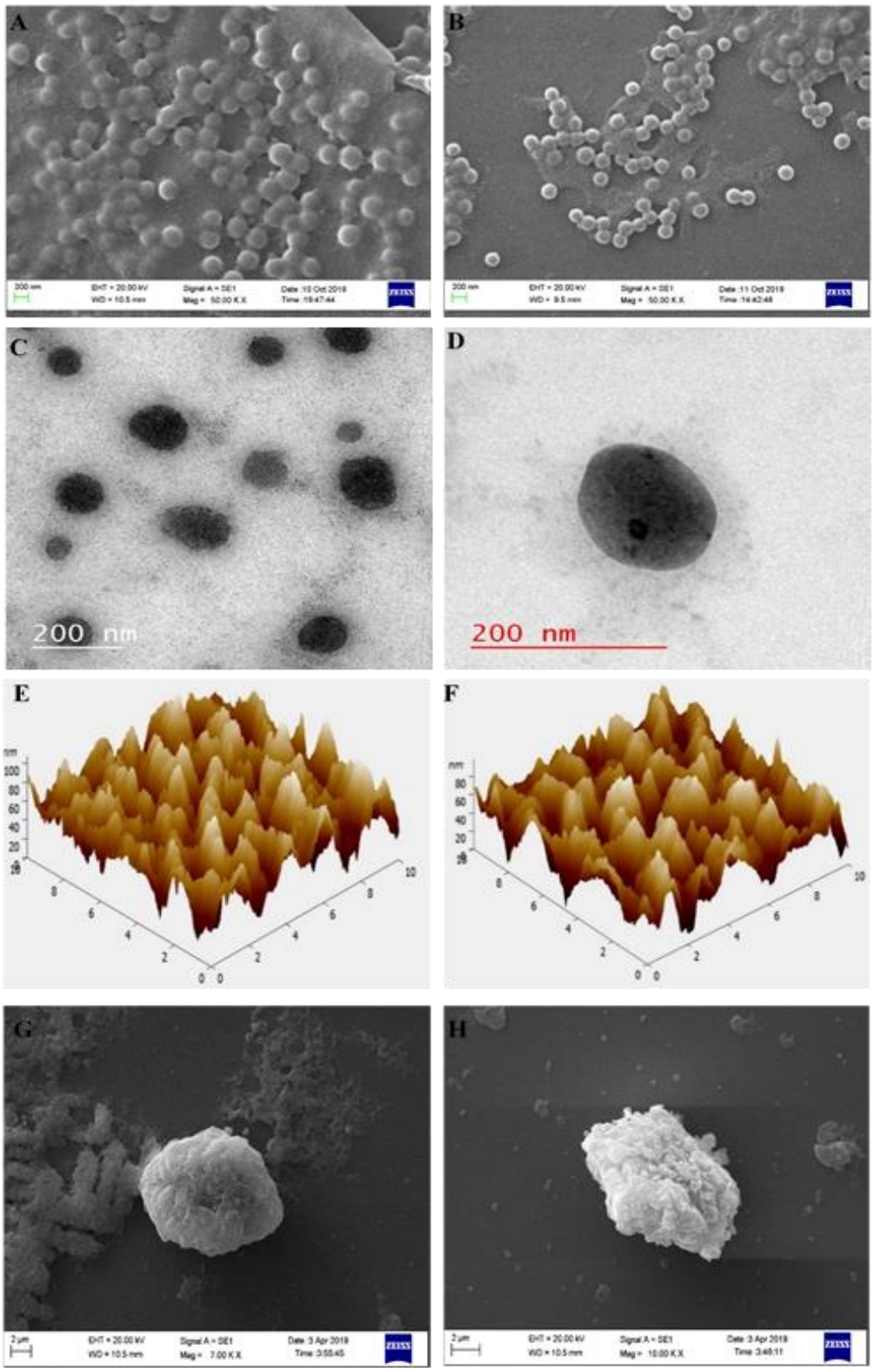

Figure 3.5. SEM micrographs (A&B) and TEM micrographs (C&D) of non-targeted NP and targeted NP respectively; AFM 3D micrographs (E&F) of non-targeted NP and targeted NP and SEM micrographs (G&H) of A549 cells treated with PBS control and CTX decorated targeted NP revealing the excellent bioadhesive behavior of targeted NP on the cell surface.

3.5.4. In-vitro studies

3.5.4.1. Drug release study

The prepared non-targeted and targeted NP were screened for release trends in different pH, i.e., pH 5.5 (pH within the cancer cell endosomes) and pH 7.4 (physiological pH). These formulations demonstrated a pH-sensitive drug release (figure 3.6). Approximately 90 % of DTX was released from Docel^{TM} within 2 h owing to its micellar form. The drug release was found to be pH-dependent. This might be attributed to the presence of amino groups in protonated state on chitosan at lower pH, which allowed DTX to diffuse quickly from the NP possibly by augmented electro-static repulsive nature. Indeed, the faster release of anti-cancer drugs from NP at lower pH will be promising in killing cancer cells with an inherent acidic environment.

3.5.4.2. Qualitative cellular uptake study

Figure 3.7.A depicts the fluorescence micrographs of A549 cells treated with CM6 loaded non-targeted and targeted NP and free CM6 and figure 3.8.A depicts the comparision of mean fluorescence intensity produced by cells after treatment. The mean fluorescence intensity produced by CTX pre-treated cells on treatment with targeted formulation was significantly low as all the EGF receptors were occupied with pretreated CTX.

Table 3.3. Physicochemical and *in-vitro* release data of non-targeted and targeted NP

Formulation	PS (nm)	ZP (mV)	PDI	EE (%w/w)	% CTX	CDR at pH 5.5	CDR at pH 7.4
Simple CS-NP	148.47±4.87	16.77±1.37	0.31±0.02	71.46±0.461	--	89.47±2.659	76.19±5.582
Non-targeted CS- NP	152.59±3.90	13.84 ± 0.93	0.37±0.01	70.8 ± 0.812	--	95.34±0.864	82.61±0.763
Targeted CS-CTX-NP	180.63±5.21	11.02 ± 0.86	0.34±0.05	74.42 ± 0.57	78.44±3.65	96.72±0.925	71.07±0.506
Non-targeted CS-C6-NP	158.12±6.59	17.38±0.72	0.29±0.04	84.0 ± 1.53	--	--	--
Targeted CS-C6- CTX-NP	177.43±11.9	14.9±0.35	0.32±0.03	88.6 ± 2.36	75.81±5.67	--	--

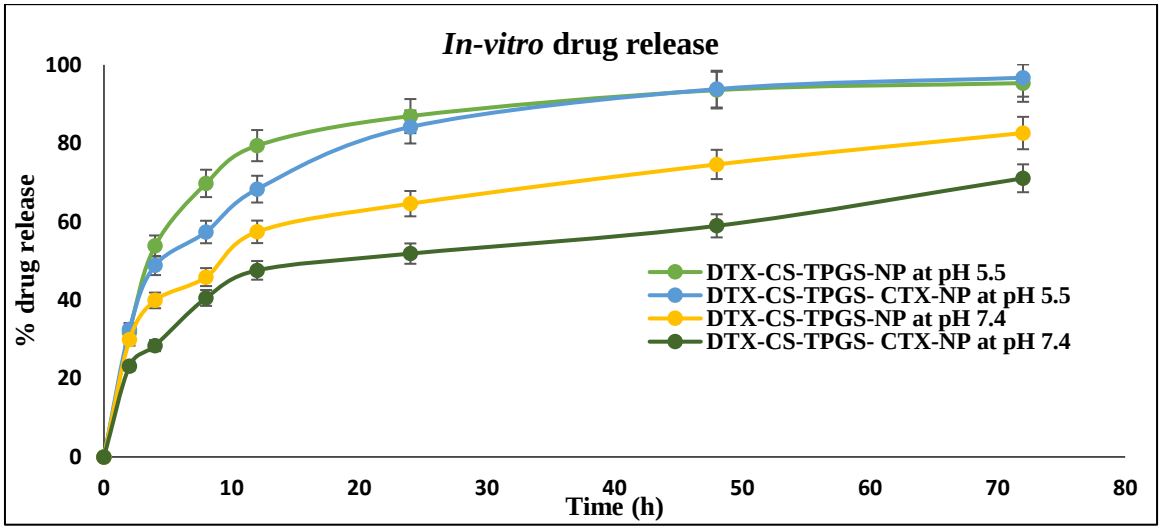

Figure 3.6. Comparative *in-vitro* drug release from non-targeted and targeted NP at pH 5.5 and pH 7.4

Non-targeted NP have produced significantly lesser fluorescence compared to the targeted NP which might be attributed to enhanced uptake of these NP through EGFR mediated endocytosis. Also, the cells treated with free CM6 displayed too low fluorescence when compared to that of the formulations.

3.5.4.3. Time-dependent cellular uptake study

Incubation of A549 cells with Free CM6, CM6- CS-TPGS-NP, and CM6-CS-TPGS-CTX-NPs (5 µg/ml of CM6) was done in the 6 well plates. The fluorescence microscopy images of incubated cells at different time intervals are depicted in figure 3.7.B. The fluorescence emitted by CM6 loaded targeted NP is far more superior to that is emitted by the free CM6 or CM6 loaded non-targeted NP.

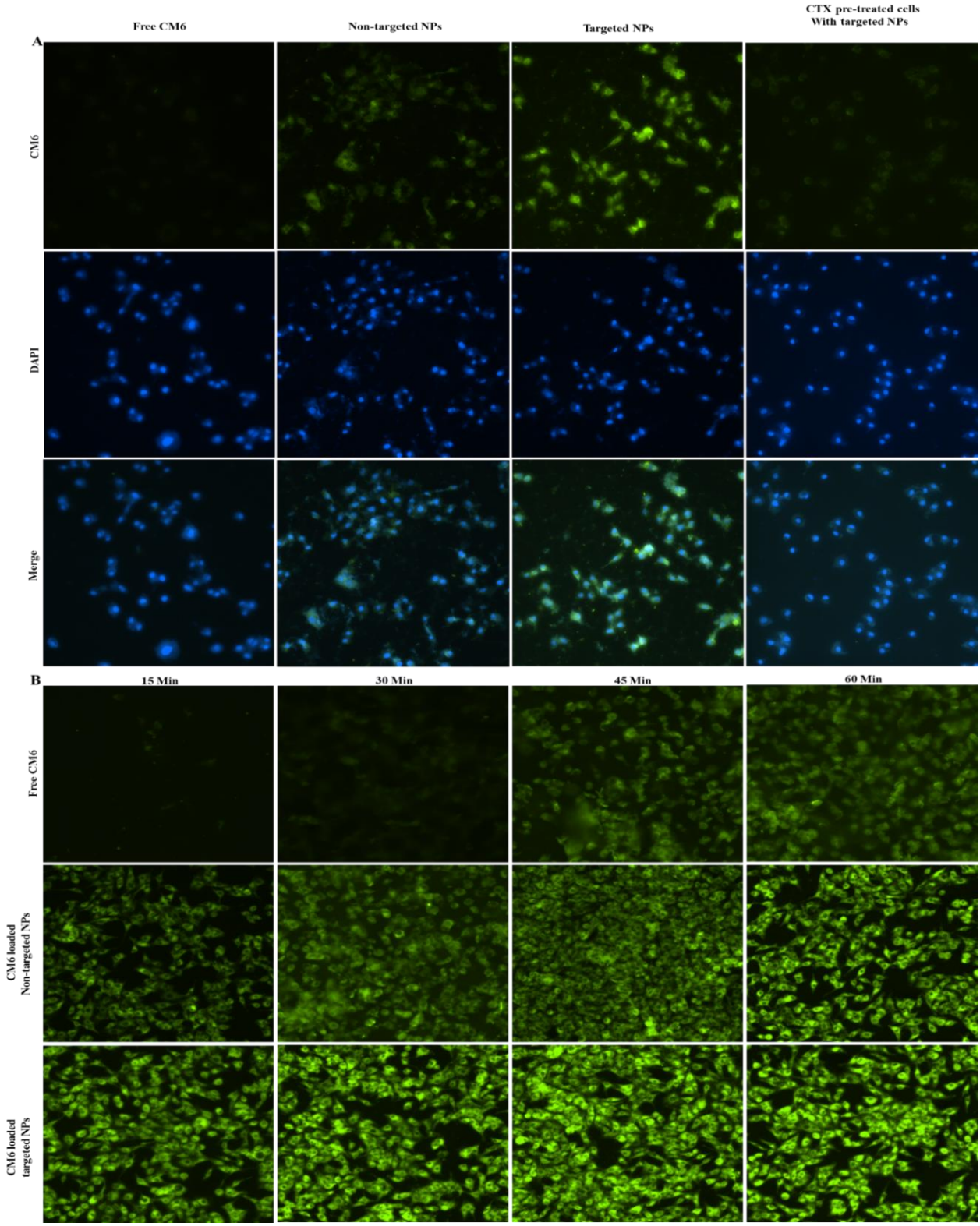

Figure 3.7. Fluorescence micrographs showing **A)** qualitative uptake of free CM6, CM6 loaded non-targeted and targeted NP by DAPI stained A549 cells; **B)** time-dependent uptake of free CM6, CM6 loaded non-targeted and targeted NP by A549 cells for the duration of 60min.

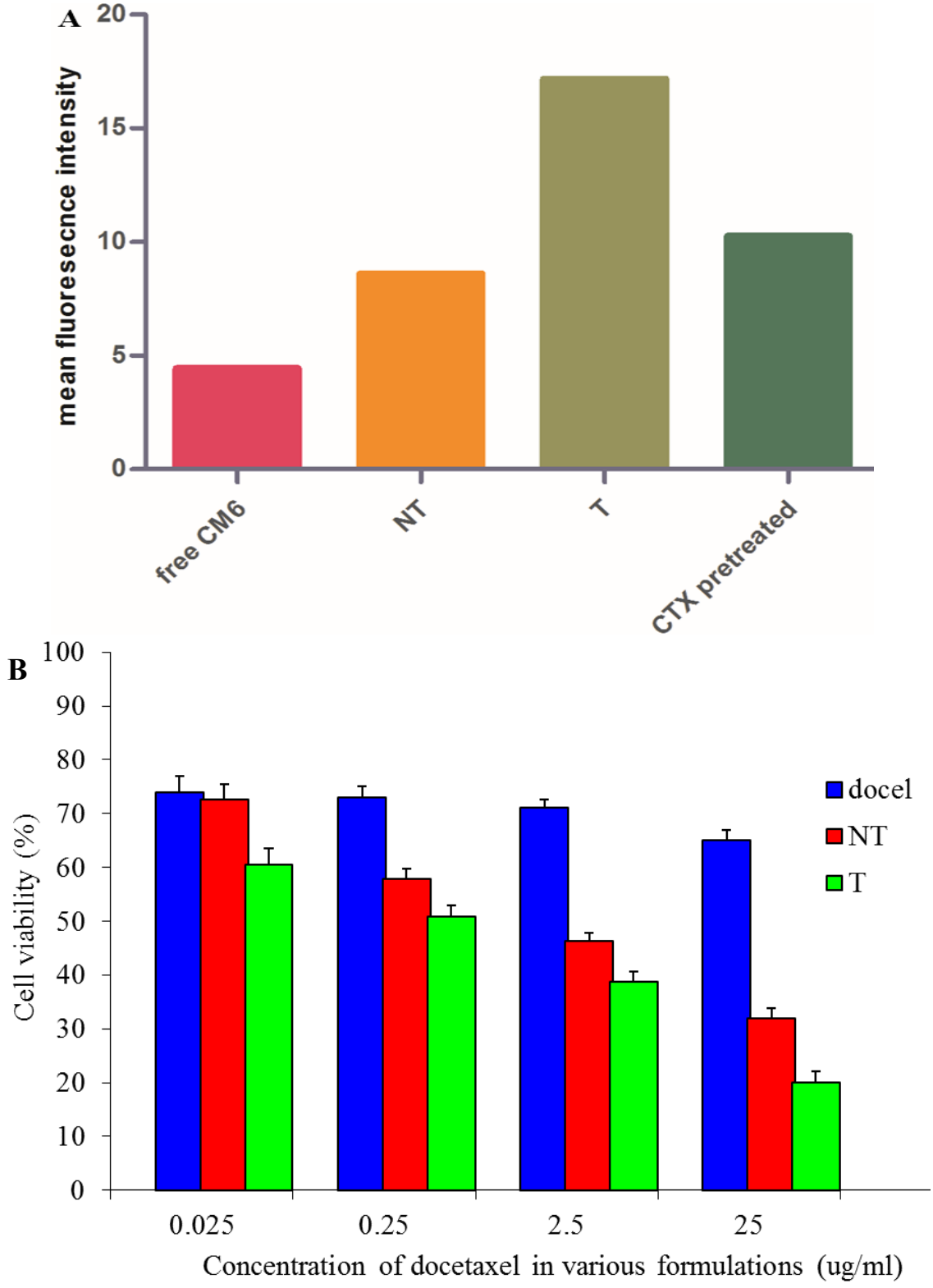

Figure 3.8. A) comparison of mean fluorescence intensity produced by A549 cells after uptake of free CM6, CM6 loaded non-targeted and targeted NP**, B)** Graph showing comparative percent cell viability against different equivalent concentrations of DTX for Docel^{TM}, non-targeted and targeted NP

3.5.4.4. Cytotoxicity studies in A549 *cells*

The cytotoxicity of prepared NP was evaluated and the results are shown in figure 3.8.B, which indicated that targeted NP elicited superior cytotoxicity than non-targeted NP and Docel™. This substantial increment in the cytotoxicity by targeted NP might be accredited to the augmented particle uptake by cells through bioadhesion along with the sustained release of DTX in addition to EGFR mediated endocytosis as compared with that of non-targeted NP and standard Docel™.

3.5.4.5. Wound healing assessment

The cytotoxic property was evaluated in wound healing assessment and the micrographs are depicted in figure 3.9.A. The percent scratch area is reduced to 10.56 % from an initial 46.3 % within 48 h in case of control. Whereas, in the case of non-targeted and targeted NP, it is increased to 54.33 % and 62.64 % respectively. The non-targeted and targeted NP treated wells, the cells showed changes in morphology due to the induction of apoptosis by DTX, which actually increased the percent scratch area.

3.5.4.6. Apoptosis assay

Fluorescence micrographs of DAPI and F-actin counterstained (phallandoin tetramethyl rhodamine conjugate) A549 cells, after incubation with control (PBS), non-targeted and targeted NP for 2 h, are shown in figure 3.9.B. The nuclei of untreated cells showed bright fluorescence with no significant signs of chromosome condensation and nuclear fragmentation on staining with DAPI. The cells treated with non-targeted and targeted NP and Docel™, chromosomal condensation was confirmed with conclusive nuclei segregation and fragmentation in the cells after 120 min of incubation.

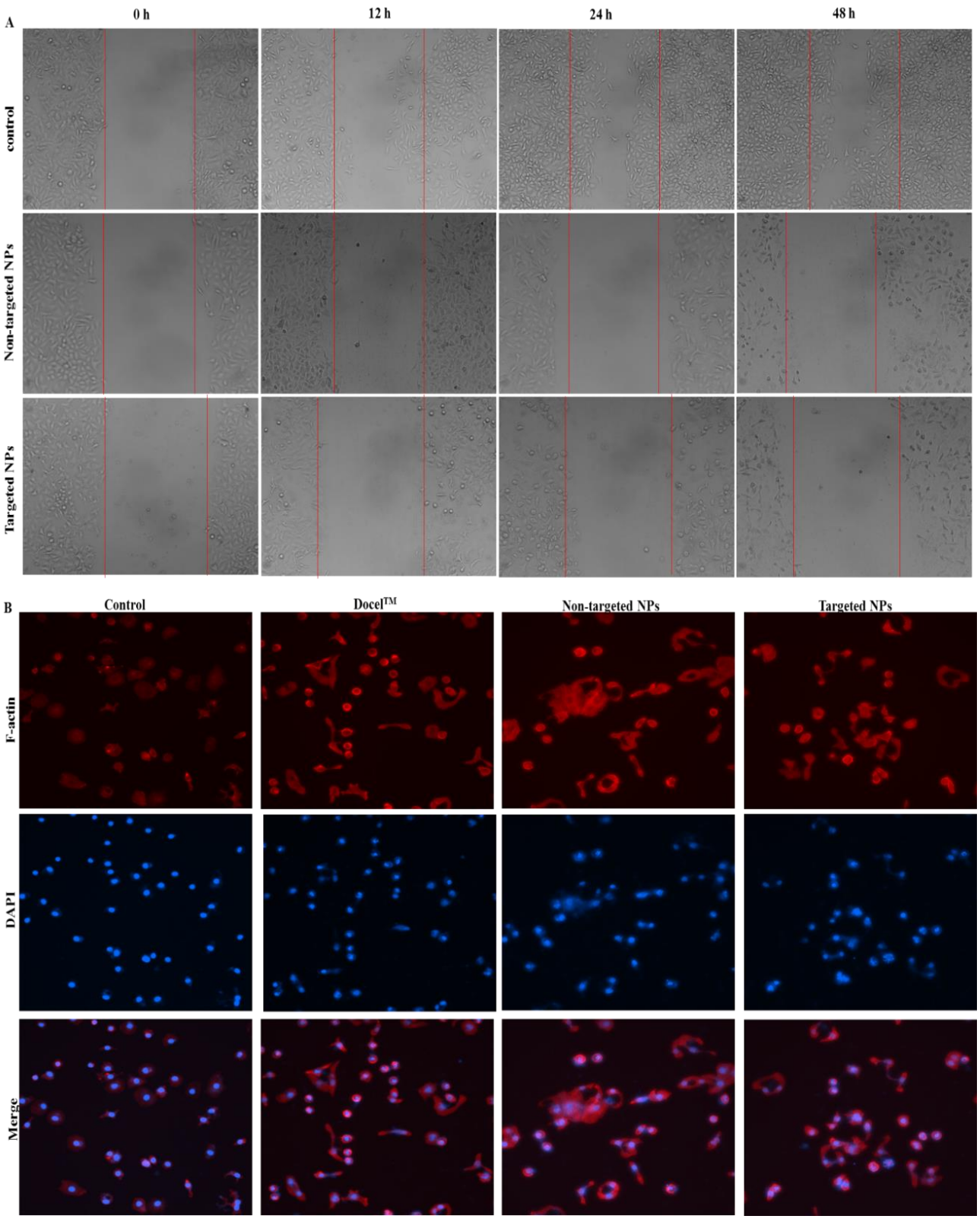

Figure 3.9. A) Light microscopic images of wound healing assessment of A549 cells treated with control (PBS), non-targeted and targeted NP; **B)** Fluorescent images of morphology assay of A549 cells treated with control (PBS), Docel™, non-targeted and targeted NP.

3.5.5. Stability studies

The stability studies on prepared formulations in terms of change in size, surface charge and EE (figure 3.10) revealed no significant effect of the said variables on their stability. A slight and insignificant increase in the size of NP was noted upon the reconstitution of freeze-dried samples and the size distribution was also found to be slightly altered. The incubation of NP in plasma has no significant effect on the size and size distribution and a slight increase in the size might be due to the natural opsonization of plasma proteins on the NP surface. The serum incubation of prepared NP has shown no significant variations in the size and size distribution. The Freeze-dried NP, upon storage at 4 °C for one month and subsequent reconstitution, were found to be stable in terms of size and size distribution.

3.5.6. In-vivo studies

3.5.6.1. Pharmacokinetic study

The plasma concentration of DTX at various time intervals was ascertained and the concentration vs. time curve was constructed (figure 3.11) following *i.v.* injection of Docel™ and DTX loaded non-targeted and CTX conjugated targeted NP to rats at the equivalent DTX concentrations (7.5 mg/kg, n = 3). The critical pharmacokinetic (PK) parameters are computed using Kinetika® software and enlisted in table 3.4. There was 1.962 and 2.694 times increment in the relative bioavailability by non-targeted and EGFR targeted NP than and the formulations achieved a three-fold extended half-life than Docel™.

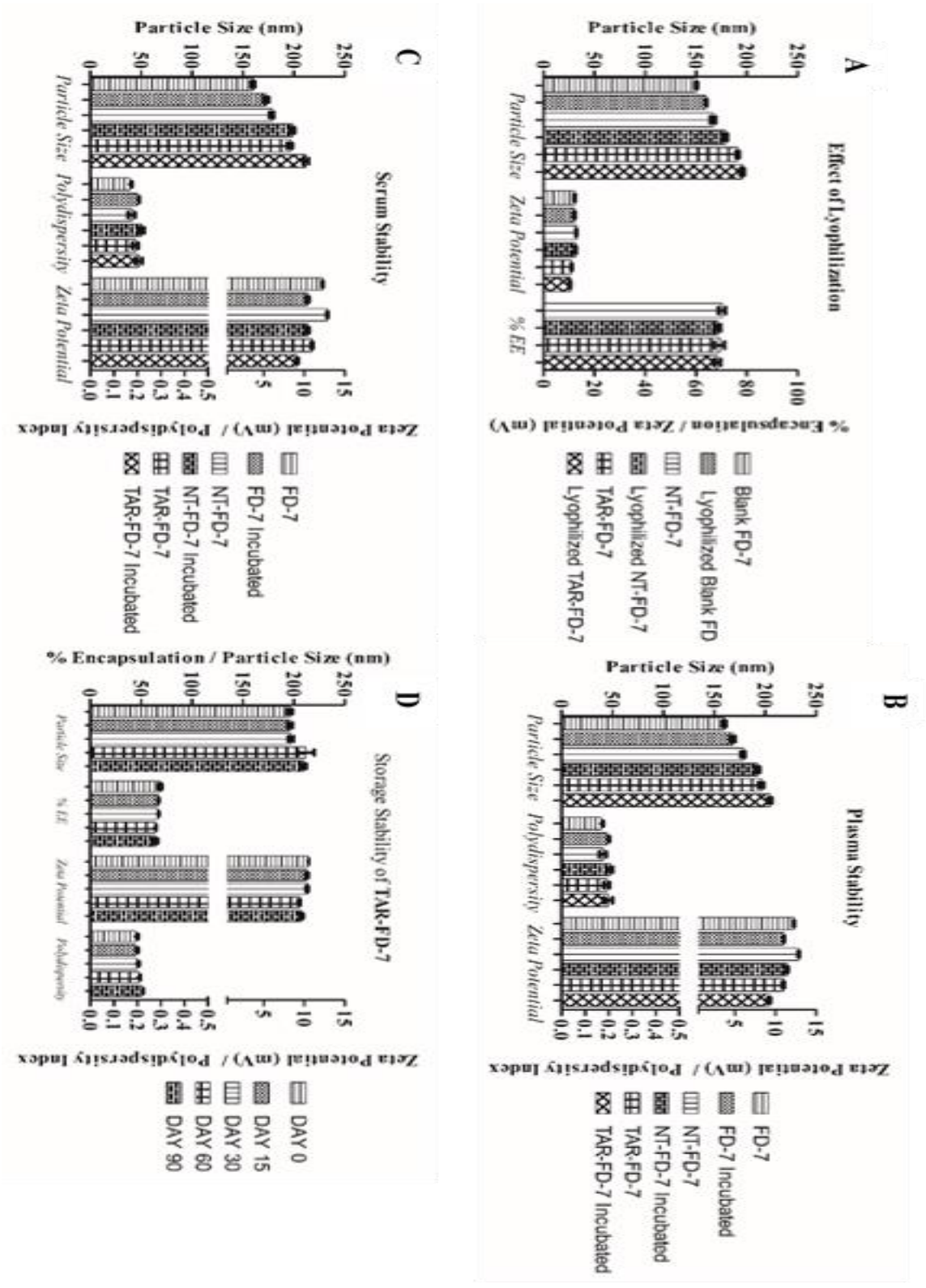

Figure 3.10. Graphs showing the effect of **A)** lyophillization, **B)** plasma incubation, **C)** serum incubation and **D)** storage on particle size, Polydispersity, zeta potential of NP

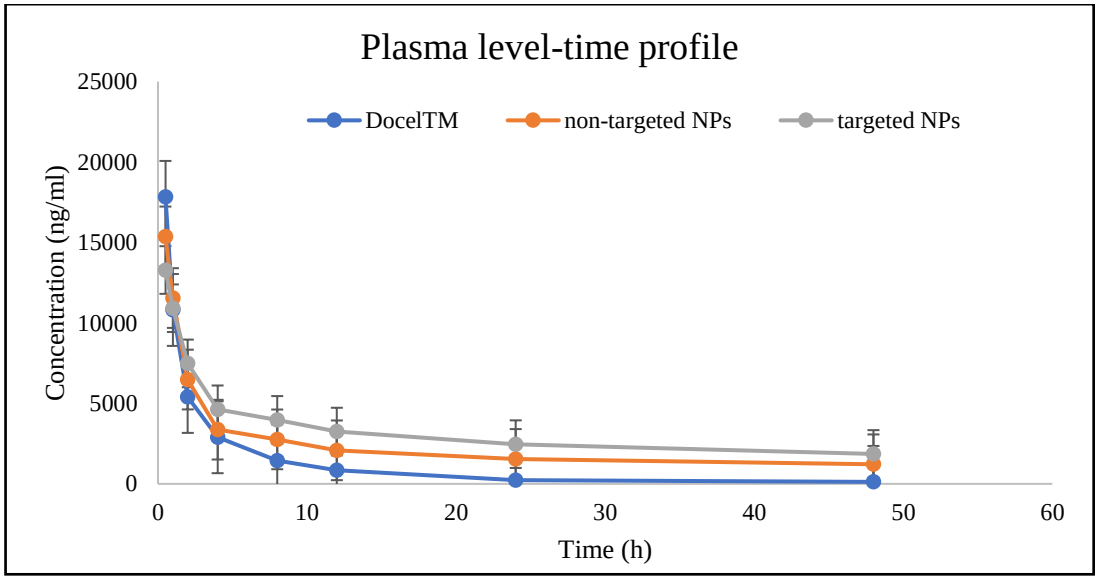

Figure 3.11. Plasma level-time profile of Docel™, non-targeted and targeted NP constructed from plasma samples analyzed by reverse-phase HPLC

Even, the other vital parameters such as AUC and MRT were ameliorated for both the NP than Docel™, which was better than the results of previous studies. From table 3.4, it can be seen that Docel™ plasma circulation time or half-life was quite brief due to faster DTX release. On the contrary, both the non-targeted and targeted NP demonstrated longer plasma circulation times.

Table 3.4. Comparison of various critical pharmacokinetic parameters of non-targeted and targeted NP with respect to Docel™

Pharmacokinetic Parameters	Docel™	Non-targeted NP	Targeted NP
$T_{1/2}$ (h)	10.086±1.06	48.134±1.309	49.490±2.386
MRT (h)	8.844±0.779	59.85±0.645	61.05±0.722
V_d (l/Kg)	0.4209	0.4877	0.5643
Cl_T (l/Kg.h)	0.09853	0.03877	0.02745
$AUC_{(0-\infty)}$ (ng.h/ml)	56235±372.37	110371±249.01	151546±213.69
F_R	--	1.962	2.694

3.5.6.2. Histopathology study in rats

The histopathological evaluation of prepared NP on the vital organs like heart, lungs, liver and kidney were evaluated by observing the histological variations in these tissues by staining their thin sections with hemotoxylin-eosin (H&E) post treatment with NP and the resulting images are depicted in figure 3.12. The saline-treated control group demonstrated no pathological lesions in the heart, lung, liver, and kidney. But the non-targeted NP treated group showed fewer pathological lesions in the heart, lung, liver, and kidney when compared to that caused by standard Docel^{TM}. Even in the targeted NP treated group, fewer lesions were observed in these vital organs when compared with those produced by Docel^{TM}, which established the safety of these NP [11].

3.5.6.3. Anticancer efficacy of nanoformulations

Figure 3.13 depicts the histological sections of benzo(a)pyrene-induced NSCLC and corresponding ImageJ® processed images of H&E stained after treatments As seen from the images, the model control showed the well-differentiated adenocarcinoma with multifocal origin from the bronchioles. The cells have been presented with characteristic polygonal appearance with large spherical or sometimes oval and vesicular nuclei and vacuolated and scanty cytoplasm. Following treatments, six different areas from each color deconvoluted image were selected and the number of particles (nuclei) were counted. One way ANOVA was used to arrive at statistically meaningful comparisons. The typical values are depicted in figure 3.14.A. The Kaplan-Meier survival analysis was done to evaluate the mean survival rate of the B(a)P induced lung cancer mice post-treatments and the same is depicted in figure 3.14.B.

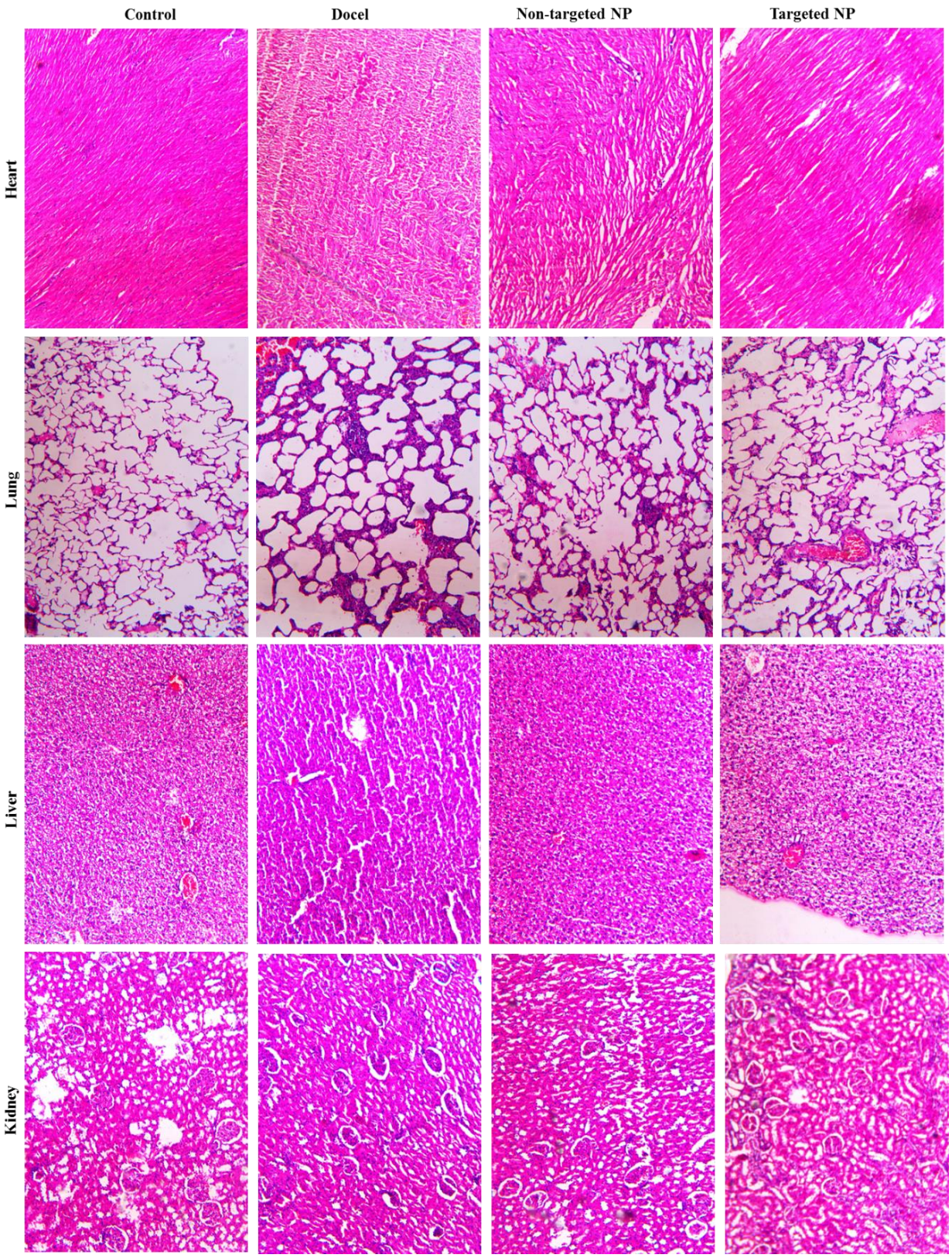

Figure 3.12. Histological images after H&E staining of the sections of vital organs such as heart, lung, liver, and kidney of rats after treatment with control, Docel^{TM}, non-targeted & targeted formulations

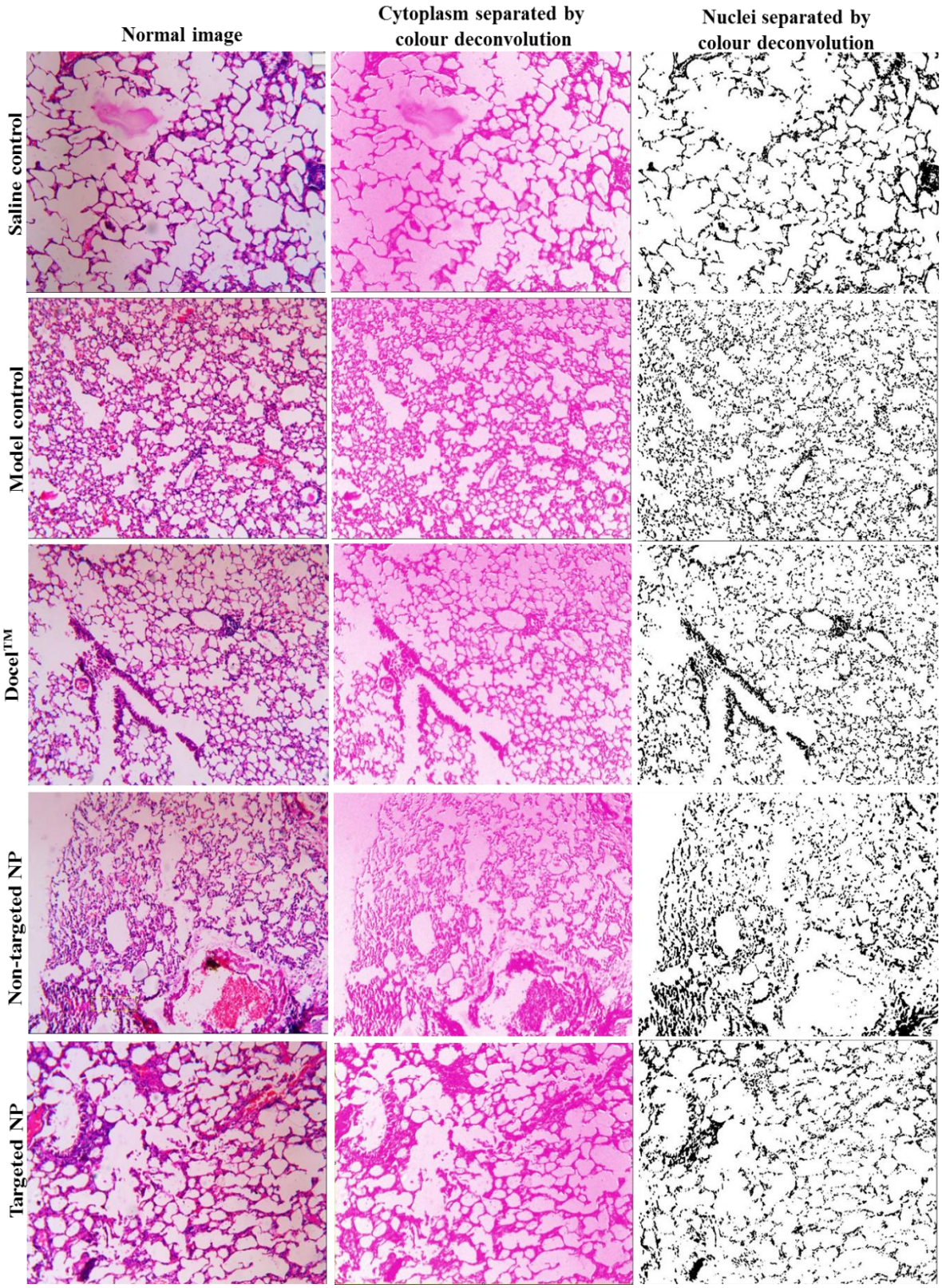

Figure 3.13. Colour deconvoluted images of the H&E stained histological sections of lung cancer tissues by ImageJ® after treatment with control, Docel™, non-targeted & targeted formulations

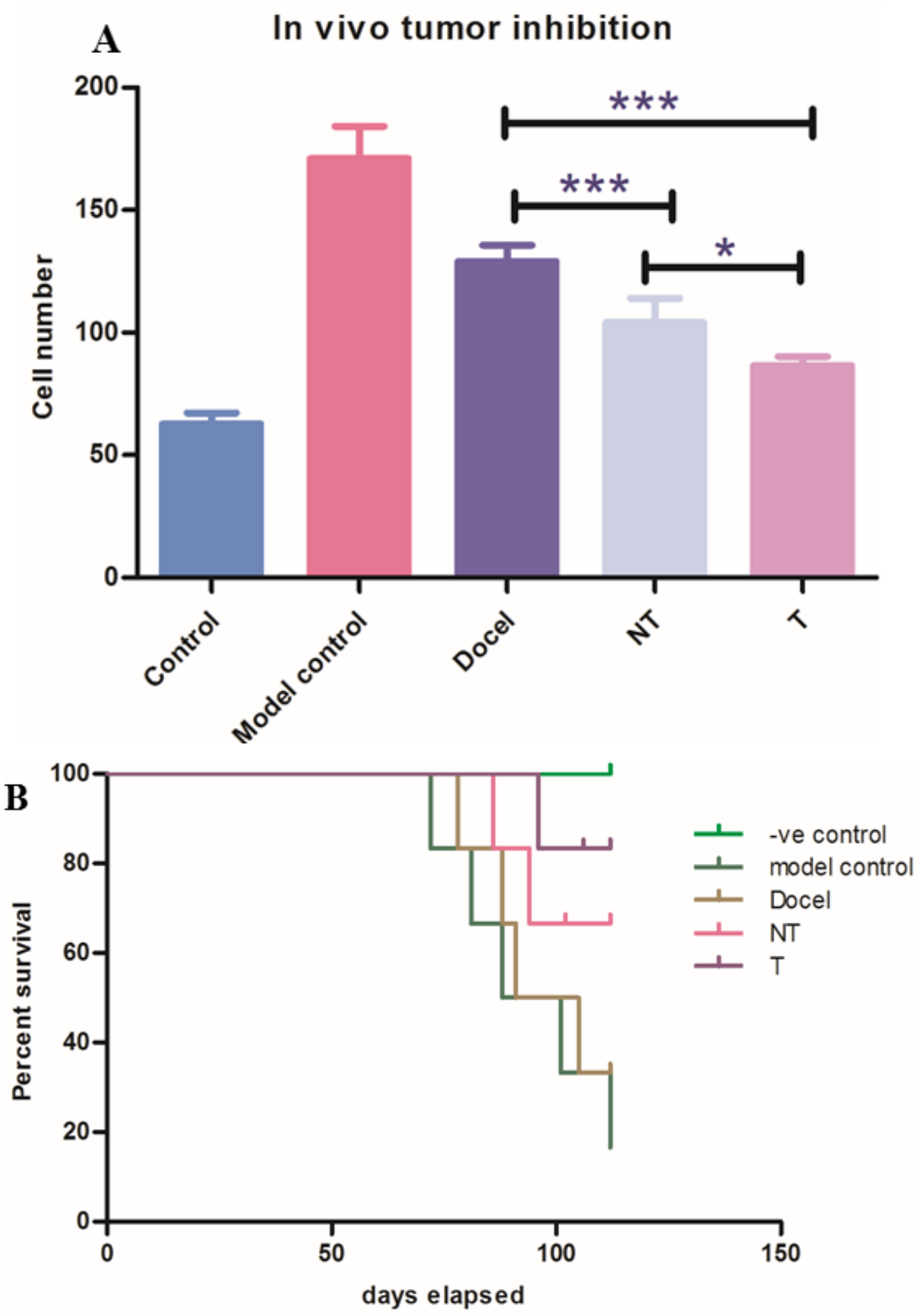

Figure 3.14. A) Graph showing the comparative *in-vivo* tumor inhibition by Docel™, non-targeted and targeted formulations in comparison to saline control and Model control. (***P<0.0001, *P<0.05), **B)** Kaplan-Meier survival analysis of mice treated with negative control, model control, non-targeted, targeted NP and Docel™.

It can be inferred from the results that a significant reduction in the cell number and tumor growth was caused by non-targeted and targeted NP in comparison to Docel^{TM} and, all the treatments have significantly reduced the tumor number in contrast to model control. Also targeted NP, compared to the non-targeted NP, caused a significant reduction in cancer cell numbers. Even non-targeted NP also showed comparable efficacy due to EPR effect in addition to bioadhesion and presence of amorphous form of drug embedded in the biodegradable matrix. The Kaplan-Meier survival analysis showed that the percent survival of mice treated with non-targeted and targeted formulations was significantly prolonged as compared with model control.

3.6. Conclusion

Chitosan-based EGFR targeted bioadhesive nanomedicine of DTX was successfully formulated by the QBD approach by using minimum material and resources. A preliminary physicochemical demonstrated promising results. XRD study revealed the amorphous state of DTX within the NP. The surface chemistry by XPS confirmed the conjugation of CTX on to the surface of targeted NP. *In-vitro* drug release studies indicated a pH-dependent drug release with a faster release rate at pH 5.5. *In-vitro* cell culture studies on A549 have confirmed that CM6 loaded targeted NP displayed superior uptake. The cytotoxicity produced by targeted NP was significantly higher than other treatments. SEM micrographs of treated cells showed that NP have adhered in large numbers to the cell surface. The *in-vitro* apoptosis study demonstrated a superior effect with targeted NP. All the pharmacokinetic parameters were found to be superior for targeted NP than non-targeted NP and Docel^{TM}. Histopathological evaluation of vital organs has revealed minor lesions compared to that of Docel^{TM} which confirmed their safety. *In-vivo* tumor inhibition studies on B(a)P induced lung cancer sections of mice

that were processed with ImageJ® have also stated that cell number was reduced significantly ($P<0.05$) by targeted NP as compared with non-targeted NP and both the formulations have demonstrated superior anti-cancer effect ($P<0.0001$) than Docel™.